OXFORD

Human Molecular Genetics, 2017, Vol. 26, No. 14 2732–2746

doi: 10.1093/hmg/ddx160
Advance Access Publication Date: 27 April 2017
Original Article

ORIGINAL ARTICLE

Post-transcriptional regulation of FUS and EWS protein expression by miR-141 during neural differentiation

Francesca Svetoni[1,2,†], Elisa De Paola[1,2,†], Piergiorgio La Rosa[2,3], Neri Mercatelli[1,2], Daniela Caporossi[1], Claudio Sette[2,3] and Maria Paola Paronetto[1,2]

[1]Department of Movement, Human and Health Sciences, University of Rome "Foro Italico", 00135 Rome, Italy, [2]Laboratories of Cellular and Molecular Neurobiology and of Neuroembryology, Fondazione Santa Lucia, 00143 Rome, Italy and [3]Department of Biomedicine and Prevention, University of Rome "Tor Vergata", Rome, Italy

*To whom correspondence should be addressed. Tel: +3906501703218; Email: mariapaola.paronetto@uniroma4.it

Abstract

Brain development involves proliferation, migration and specification of neural progenitor cells, culminating in neuronal circuit formation. Mounting evidence indicates that improper regulation of RNA binding proteins (RBPs), including members of the FET (FUS, EWS, TAF15) family, results in defective cortical development and/or neurodegenerative disorders. However, in spite of their physiological relevance, the precise pattern of FET protein expression in developing neurons is largely unknown. Herein, we found that FUS, EWS and TAF15 expression is differentially regulated during brain development, both in time and in space. In particular, our study identifies a fine-tuned regulation of FUS and EWS during neuronal differentiation, whereas TAF15 appears to be more constitutively expressed. Mechanistically FUS and EWS protein expression is regulated at the post-transcriptional level during neuron differentiation and brain development. Moreover, we identified miR-141 as a key regulator of these FET proteins that modulate their expression levels in differentiating neuronal cells. Thus, our studies uncover a novel link between post-transcriptional regulation of FET proteins expression and neurogenesis.

Introduction

The FET family of DNA and RNA binding proteins comprises FUS/TLS (fused in sarcoma/translocated in liposarcoma, from herein named FUS), EWS (Ewing Sarcoma protein), and TAF15 (TATA box binding protein associated factor 15) (1–3). FET proteins are characterized by several conserved domains, including an N-terminal Serine-Tyrosine-Glycine-Glutamine (SYGQ)-rich transcriptional trans-activating domain (4), one RNA-recognition motif (RRM), one RanBP2-type zinc-finger motif, and three Arginine-Glycine-Glycine (RGG) boxes involved in protein-protein interactions and RNA binding (2,3). They are expressed in most human tissues and mainly localize to the nucleus (5), although shuttling to the cytoplasm has been described for FUS and EWS (6). FET proteins associate with factors involved in both transcriptional regulation and RNA processing, highlighting their multilayered role in gene expression regulation (2,3). Notably, various human cancers carry chromosomal translocations generating in frame fusions of the first part of FET genes (encoding the transcription activation domain) with genes encoding transcription factors of the ETS family (7–9). The generated chimeric proteins display strong oncogenic properties and drive neoplastic transformation (3,10). For instance, EWS-ETS chimeric proteins turn on an oncogenic transcriptional program that promotes neoplastic disease collectively named Ewing sarcomas. These are aggressive, poorly differentiated neoplasm of solid bone that afflict children and young adults.

[†]These authors contributed equally to the manuscript.

Received: February 17, 2017. **Revised:** April 19, 2017. **Accepted:** April 21, 2017

Despite intensive multi-modal therapy, 70% of patients with relapsed and metastatic Ewing sarcoma still succumb to their disease (7–10). Thus, understanding the timing and spectrum of FET protein expression has strong physiological and pathological implications.

Genetic models of FET gene ablation suggested a role for FUS and EWS in brain development. In zebrafish, *ewsr1* (the gene encoding EWS) deficiency leads to reduction in the number of pro-neural cells, disorganization of neuronal networks, and embryonic lethality by 5 days post-fertilization (11). The loss of pro-neural cells in the developing central nervous system (CNS) was ascribed to abnormalities in mitotic spindles, followed by p53-mediated apoptosis (11). In the mouse, *Fus* null hippocampal neurons display abnormal spine morphology, characterized by irregularly branched dendrites and immature axons extended from the cell body (12,13). Accordingly, FUS protein is localized to the soma and dendrites of mature hippocampal pyramidal neurons. Upon activation, FUS accumulates in the spines at excitatory synapses, concomitant with increased RNA export into dendrites and translational activation of selected transcripts (12,14). These observations suggest that FUS plays a role in establishing the correct dendrite morphology and signal propagation in neurons (12–15). TAF15 was shown to regulate alternative splicing of the zeta-1 subunit of the glutamate N-methyl-D-aspartate receptor (GRIN1) in neurons, thus controlling the activity and trafficking of NMDA glutamate receptor and impacting critical neuronal RNA networks (16).

FET proteins have been recently implicated in neurological diseases (14,17–19). For instance, all three proteins localize to Huntingtin poly-glutamine intracellular aggregates in Huntington's disease (20), whereas mutations in FET genes have been implicated in Amyotrophic Lateral Sclerosis (ALS) (14). In particular, mutations in *FUS* have been identified in familial cases of ALS, resulting in neuronal ubiquitin-positive cytoplasmic inclusions (21–23). Since FUS-positive aggregates were also found in frontotemporal lobar degeneration (FTLD) patients, dysregulation of FET proteins function might also be involved in FTLD pathogenesis (24–26).

Defects in DNA repair have been extensively linked to neurodegenerative diseases (27), however, the mechanisms involved are still poorly understood. Notably, increased DNA damage was also observed in human ALS patients harboring FUS mutations (27), while EWS deficiency causes hypersensitivity to ionizing radiation (28), probably due to the role played by EWS in the regulation of alternative splicing of genes involved in the DNA damage response (29–31). Thus, dysregulation of FET proteins function might hamper mechanisms involved in the control of genome stability and contribute to the pathogenesis of neurodegenerative diseases.

In spite of the clear involvement of FET proteins in brain development and pathologies, the overall timing and pattern of expression of these proteins in the central nervous system is currently unknown. In this work, we have characterized the expression of FET proteins during mouse brain development and neural progenitor cell (NPC) differentiation. We observed that FUS and EWS proteins decrease upon neural differentiation, while TAF15 levels remain constant. Interestingly, the corresponding mRNAs were only slightly affected. To explain the underlining mechanism, we searched for miRNA-based regulation of FUS and EWS expression. We found that the decline in FUS and EWS expression is paralleled by an up-regulation of miR-141 and miR-200b during neuronal differentiation and that overexpression of miR-141, but not of miR-200b, mimics the physiological regulation. Our data highlight a fine-tuned regulation of FET protein and RNA expression during brain development and identify a post-transcriptional mechanism of control that could play a role in the pathogenesis of FET-related neurological disorders.

Results

Expression of FET proteins is markedly decreased upon brain development

Given the role played by FET proteins in RNA processing and neurodegenerative disease, we set out to investigate their expression in the developing brain. Western blot analysis showed that all FET proteins are robustly expressed in mouse embryonic brain, whereas they are differentially modulated during postnatal development (Fig. 1A). The levels of FUS and EWS proteins in the cortex peak between E15.5 and birth, whereas their expression is reduced thereafter and is minimal from 16 days post-partum (16dpp) until adulthood (Fig. 1A and B). Notably, the post-natal decline is much more pronounced for EWS than FUS. By contrast, while TAF15 initially follows the pattern of the other FET proteins, with a sharp decrease after birth, it is then expressed at higher levels in the adult (24-60dpp) brain cortex (Fig. 1A and B).

Next, we investigated the pattern of expression of FET protein in regions of the adult brain. EWS appeared the most regionalized protein, with highest expression in the cerebellum, followed by striatum and cortex, and minimal expression in the hypothalamus and hippocampus (Fig. 1C and D). On the contrary, FUS was almost equally expressed in all regions, with the exception of the hippocampus in which it was significantly reduced, whereas TAF15 expression was low only in the cortex (Fig. 1C and D). These results highlight a specific pattern of temporal and spatial expression for each FET protein during brain development, suggesting potential non-overlapping functions for this family of RBPs.

FET protein expression in differentiating NSCs

Our results suggested a higher expression of FUS and EWS during embryonic cortical development (15.5 days post coitum, dpc, E15.5). Thus, expression of both protein peaks at stages of intense neurogenesis in the developing cortex and declines after birth, when the differentiation process is almost completed (32). To confirm this finding, we isolated neural stem cells (NSCs) from 13.5 embryos (E13.5). NSCs are self-renewing cells that can differentiate into multiple neural lineages and repopulate regions of the brain both physiologically and after injury (32,33). In the presence of minimum medium supplemented with epidermal growth factor (EGF) and basic fibroblast growth factor (bFGF), NSCs maintain the ability to grow clonally and form floating spheres, even though their clonogenic potential slowly declines with in vitro passages (34,35). Immunofluorescence analysis showed that all FET proteins are expressed in undifferentiated NSCs grown in suspension (Supplementary Material, Fig. S1), which were identified using the neural progenitor marker Nestin. To investigate the subcellular localization of FET proteins, NSCs were allowed to attach onto laminin/poly-ornithine substrate. Notably, while FUS and EWS staining was present both in the nucleus and in the cytoplasm, TAF15 was exclusively localized in the nucleus of the Nestin-positive cells (Fig. 2A–C). Thus, FET proteins are co-expressed but show different subcellular localization in isolated NSCs. Notably, although all three proteins contain a nuclear localization signal (NLS) in

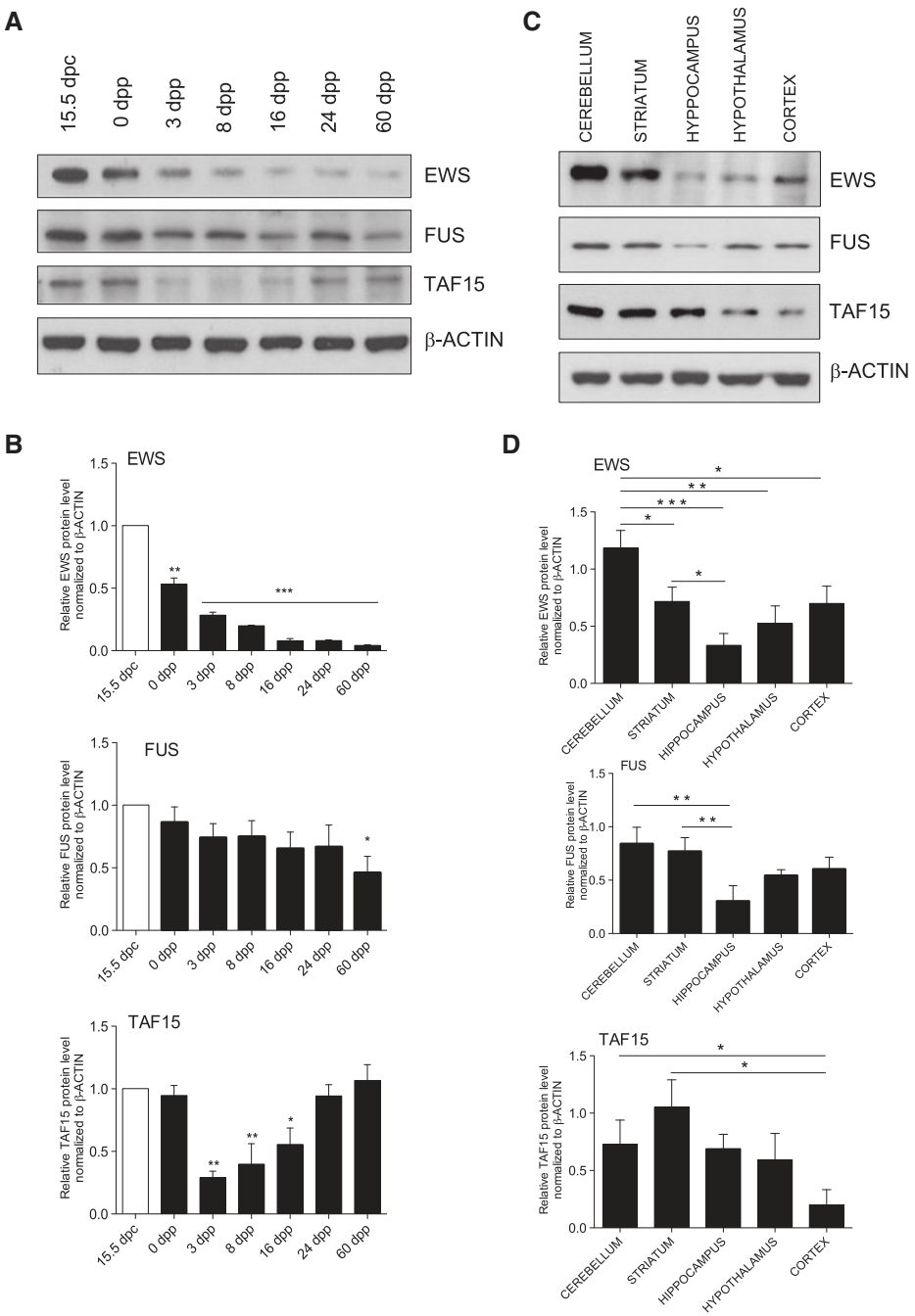

Figure 1. FET Expression in mouse brain. (**A**) FET protein expression was monitored during mouse brain development by western blot analysis in the developing mouse brain. Total extracts were normalized to β-ACTIN content. (**B**) Histograms represent the ratio between FET protein (FUS, EWS and TAF15) and β-ACTIN from three independent experiments ($n = 3$; mean ± s.d). Statistical analysis was performed by using Student's *t*-test and comparing each time point with the embryonic 15.5 dpc values. $^{*}P < 0.05$, $^{**}P < 0.01$, $^{***}P < 0.001$. (**C**) Western blot analysis of FUS, EWS and TAF15 proteins in different brain areas from 7 dpp mice. Total extracts were normalized to β-ACTIN content. (**D**) Bar graphs represent densitometric analyses of FUS, EWS and TAF15 protein expression normalized to β-ACTIN expression from three independent experiments. Histograms and error bars represent mean and standard deviation, respectively, from three independent experiments ($n = 3$; mean ± s.d). Statistical analysis was performed by using one-way Anova with Tukey's post-test. $^{*}P < 0.05$, $^{**}P < 0.01$, $^{***}P < 0.001$.

the C-terminus, a nuclear export signal could be identified only in FUS (Fig. 2D), partially explaining these differences in subcellular localization.

Upon depletion of growth factors and the addition of 1% fetal bovine serum (FBS), NSCs cease to proliferate and undergo differentiation into astrocytes, oligodendrocytes and neurons (Fig. 3A) (35,36). Under these conditions, TAF15 maintained its strong nuclear signal in astrocytes (large and spread GFAP-positive cells; Supplementary Material, Fig. 2A), while FUS and EWS expression was almost suppressed in astrocytes and remained detectable in the more undifferentiated cells (neuron-like, elongated GFAP-positive cells; Supplementary Material, Fig. S2A). Identification of the differentiating neurons by using the neuronal marker TUBB3 (βIII-tubulin) indicated that EWS expression was initially reduced in the early stages of differentiation (day 1 and 3), whereas it returned higher in the more

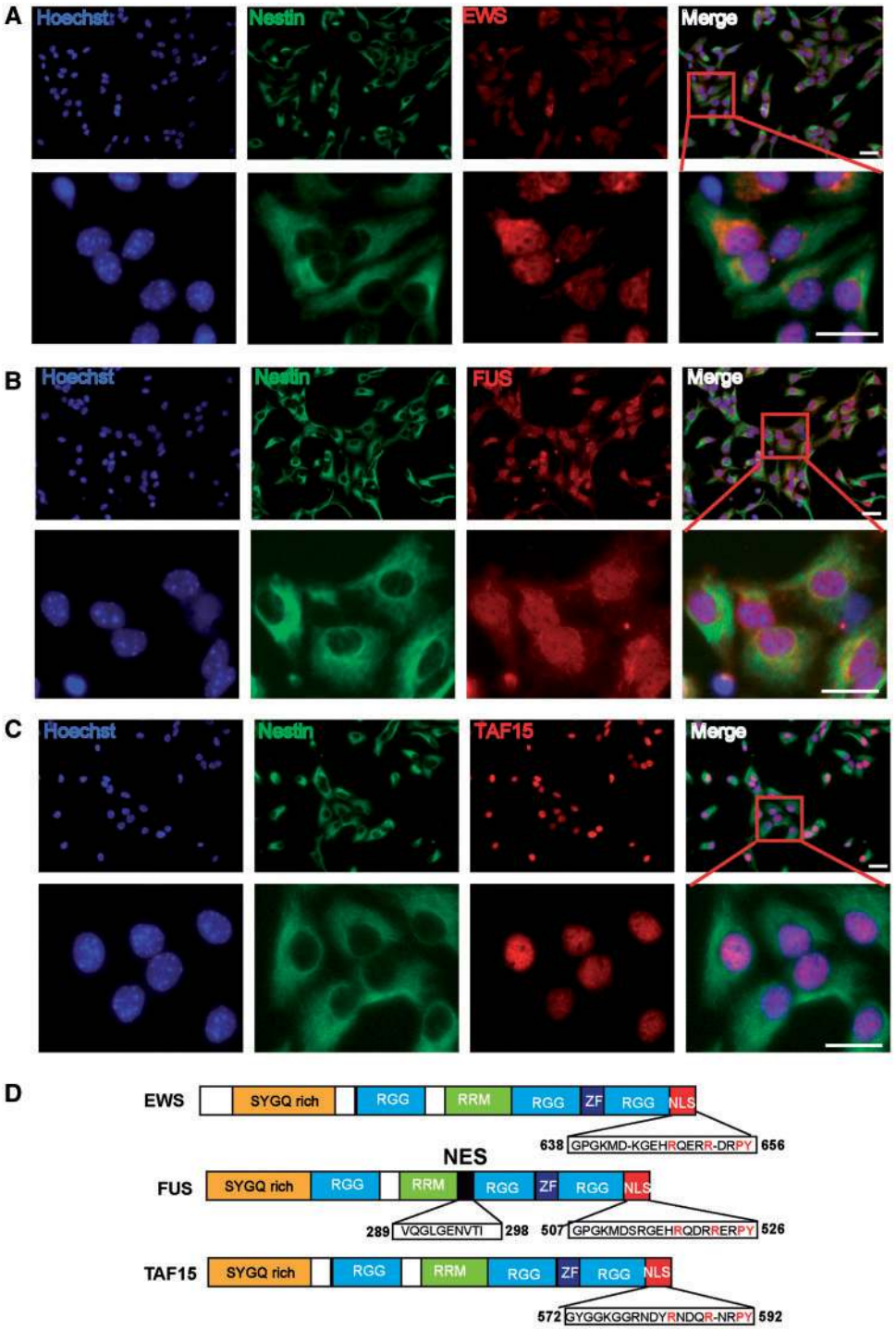

Figure 2. Immunofluorescence analysis of FET protein in NSCs. (**A–C**) FET protein expression in progenitor neural cells. Immunofluorescence analysis of progenitor NSCs stained with the precursor marker Nestin (green) and co-stained with anti-EWS, anti-FUS and anti-TAF15 (red) antibodies. DAPI was used for the DNA staining (blue). The insets show higher magnification of selected neural progenitor cells. Scale bar = 25 μm. (**D**) Schematic diagram showing the domain structure of FUS, EWS and TAF15. Sequences of the C-terminal Nuclear Localization Signal (NLS) and of the putative Nuclear Export Signal (NES) are shown in the box. SYGQ-rich = serine, tyrosine, glycine, glutamine-rich domain; RRM = RNA recognition, RGG = Arginine Gycine Glycine domain; ZnF = zinc finger. In red are shown the aminoacids essential for nuclear localization of EWS protein (41), conserved also in the other FET proteins.

mature, branched neurons at day 6 of differentiation (Fig. 3B, Supplementary Material, Fig. S2B). By contrast, FUS expression was high at day 1 of differentiation but it almost disappeared in more differentiated neurons at days 3 and 6 (Fig. 3C; Supplementary Material, Fig. 2B). Under the same conditions, no major changes in TAF15 expression were observed (Fig. 3D).

In order to quantitatively evaluate the changes in FET protein expression during neural differentiation, we performed western blot analyses of NSCs induced to differentiate for 1, 3 or

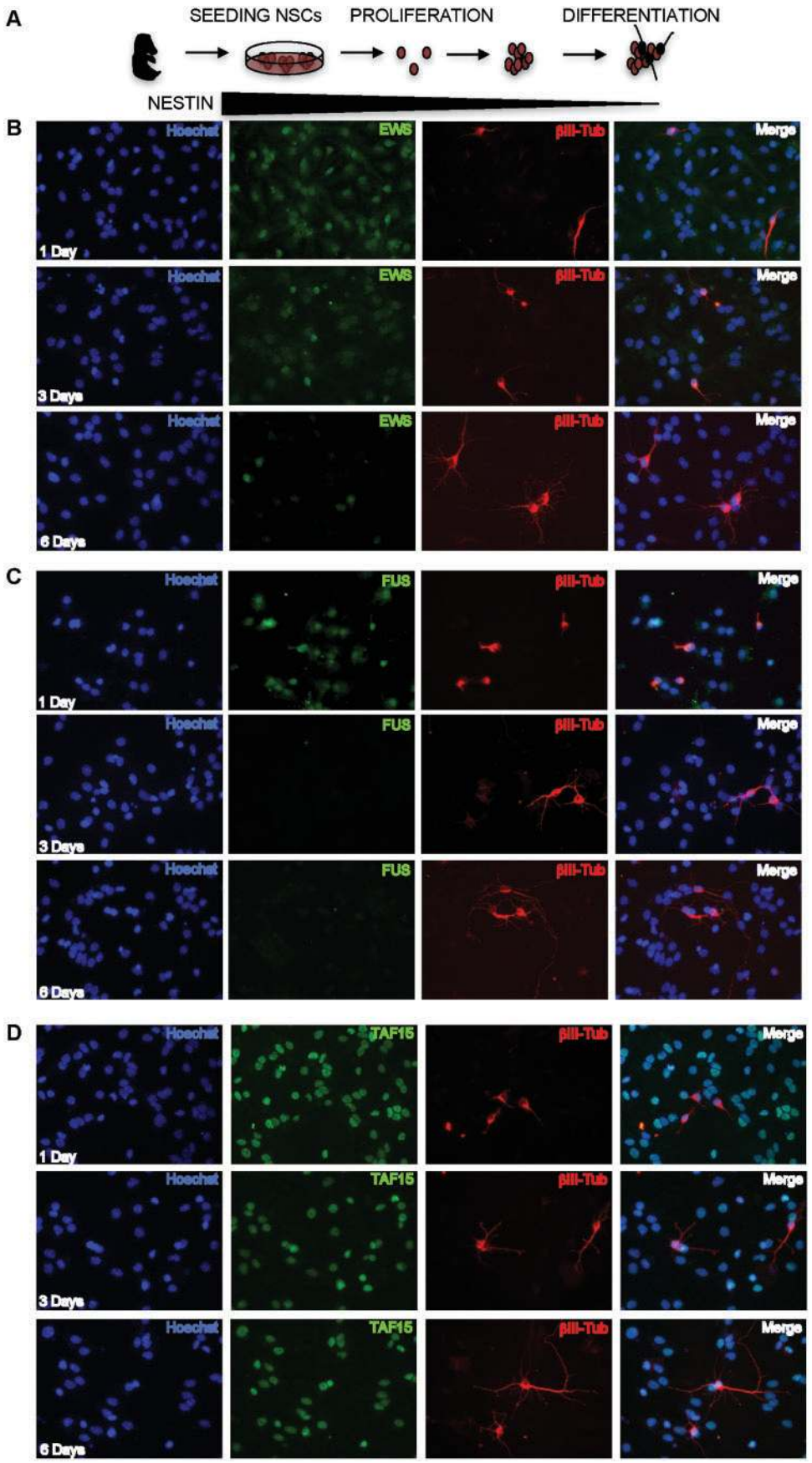

Figure 3. FET expression in NSCs. (**A**) Scheme of the protocol used for NSCs purification, proliferation and differentiation. Proliferating neural progenitors were deprived of EGF and b-FGF, and supplemented with 1% FCS. After 1, 3 and 6 days in differentiation medium cells were stained with the neuronal marker βIII-tubulin (red) and co-stained with anti-EWS (**B**), anti-FUS (**C**) or anti-TAF15 (**D**) (green) antibodies. DAPI was used for the DNA staining (blue). Scale bar = 20 μm.

6 days. FUS and EWS expression was dramatically decreased upon differentiation of NSCs, while TAF15 protein expression remained constant (Fig. 4A). These results suggest that the decrease in EWS expression during NSCs differentiation is associated, at least in part, with astrocyte differentiation, while EWS protein is partially re-expressed in neuronal cells at 6 days of differentiation (Fig. 3). On the contrary, the decrease in FUS expression can be ascribed to differentiation in both neurons and astrocytes. Moreover, subcellular fractionation experiments showed that FUS protein was partially localized also in the cytoplasm in NSCs, where it accumulated after one day of differentiation, before disappearing at day 3 (Fig. 4B and C). On the contrary, EWS was present both in the nucleus and in the cytoplasm in undifferentiated NSCs and after one day of differentiation, whereas it was confined in the nucleus at day 3 and 6 (Fig. 4B and C). TAF15 maintained its strong nuclear expression during the whole time-course (Fig. 4B and C). Notably, quantitative real time PCR (qPCR) analysis documented that *Fus, Ewsr1 and Taf15* transcripts were not significantly affected by the differentiation process (Fig. 4D). These findings indicate a different timing and cell-specific expression/localization of FET proteins during NSC differentiation and suggest a post-transcriptional regulation of *Ews* and *Fus* transcripts.

FET protein expression in differentiating SH-SY5Y cells

Since NSCs differentiate in other cell types in addition to neurons (34–36), which do not always express FET proteins as the neurons (Fig. 3, Supplementary Material, Fig. S2), we set out to investigate the expression of FET proteins during neuron differentiation in a more homogeneous population. To this end, we took advantage of human SH-SY5Y neuroblastoma cells, which maintain their potential for neuronal differentiation upon treatment with all-trans-retinoic-acid (RA) in culture (37). Using TUBB3 staining to assess morphological features of neurons, we confirmed that treatment with RA induced branching of long and interconnected neurites from 1 to 6 days of differentiation, whereas control cells did not show neurite outgrowth (Fig. 5A and B). Western blot analyses showed that FET proteins were differentially regulated during this process. Expression of FUS and EWS was significantly reduced during neuronal differentiation. However, while FUS almost completely disappeared after 6 days, EWS expression persisted, albeit at a lower level than in undifferentiated cells, whereas TAF15 showed no significant changes in protein expression (Fig. 5C and D). Notably, as also observed for NSC differentiation, qPCR analyses indicated that *FUS* and *EWSR1* mRNAs did not parallel protein expression levels. Indeed, no significant reduction in transcript levels was observed at day 3, when the corresponding proteins were markedly reduced, whereas a small decline in mRNA expression was significantly detected only after 6 days (Fig. 5E). These results confirm a fine-tuned and specific regulation of expression for the FET proteins during neural differentiation in human cells, and highlight the hypothesis of a post-transcriptional mechanism of regulation leading to the initial reduction of FUS and EWS protein levels.

miR-141 drives FUS and EWS downregulation during neural differentiation

Mechanistically, mRNA/protein expression decoupling is often linked to translational repression by specific microRNAs (miRNAs) (38). Bioinformatics search for miRNA-responsive elements in the FUS and EWS 3'-UTR predicted potential binding sites for miR-141/miR-200a, miR-200b/c and miR-340 (Fig. 6A). MiR-141 and miR-200a share the same seed sequence and belong to the miR-200 family (39), which includes five miRNAs (miR-200a, miR-200b, miR-200c, miR-429 and miR-141) encoded by two independent *loci*: the miR-200b/200a/429 cluster on chromosome 1 and the miR-200c/141 cluster on chromosome 12. Members of this family are of particular interest, because they are downregulated during tumor progression and act as key regulators of epithelial-to-mesenchymal transition (40).

We asked if the expression of miR-141, miR-200b and miR-340 was affected during SH-SY5Y cell differentiation, concomitantly with EWS and FUS downregulation. qPCR analyses revealed that miR-141 and miR-200b are strongly upregulated during neural differentiation (Fig. 6B), as well as during postnatal mouse brain development (Supplementary Material, Fig. S3A), while miR-340, predicted to target only the 3'UTR of *EWSR1* by our *in silico* analysis, was only slightly upregulated after three days of RA-induced differentiation (Fig. 6B). Remarkably, miR-141 and miR-200b upregulation anticipated the downregulation of FUS and EWS protein, suggesting that they might be involved in post-transcriptional regulation of their expression. To test this hypothesis, we transfected miR-141 and miR-200b mimics in SH-SY5Y cells. miRNA mimic expression was confirmed by qPCR analysis after 36 h from transfection (Fig. 6C), whereas the effect on FET protein expression was evaluated after 72 h by western blot analysis. Transfection of the miR-141 mimic caused a significant downregulation of EWS and FUS expression, while miR-200b did not significantly modulate it (Fig. 6D and E, Supplementary Material, Fig. S3B–D).

Gene ontology analysis of the putative targets of miR-141 highlighted enrichment in functional categories involved in neuron differentiation and RNA regulation (Fig. 7A), suggesting that this miRNA might have a broader function. To test this hypothesis, we transfected an inhibitor of miR-141 (antagomiR-141) before induction of neuronal differentiation. Remarkably, transfection of the antagomiR-141 abolished the onset of differentiation of SH-SY5Y by RA at two days upon treatment (Fig. 7B and C), together with suppressing downregulation of FUS and EWS (Fig. 7D). These results suggest that miR-141 controls a general neuron differentiation program that includes concomitant downregulation of FUS and EWS expression.

To verify the direct role of miR-141 on the regulation of FUS and EWS transcripts, we cloned their 3' untranslated regions (3'UTRs) in a reporter vector downstream of the luciferase coding sequence. Transfection of the miR-141 mimic in SH-SY5Y cells significantly reduced luciferase activity associated with FUS 3'UTR, while it had no effect on EWS (Supplementary Material, Fig. S4A and B), suggesting an indirect or additional mechanism. Triple nucleotide mutation in the seed sequence of FUS 3'UTR completely abolished mimic-141 regulation (Supplementary Material, Fig. S4A), confirming direct action on this target.

Collectively, our results describe a fine-tuned regulation of FUS and EWS expression during neural differentiation, which is operated, at least in part, by a miR-141-based mechanism of post-transcriptional regulation.

Discussion

FET proteins play key roles in the central nervous system and dysregulation of their expression or function has been implicated in neurodegenerative diseases (14). However, the regulation of their expression during brain development is not

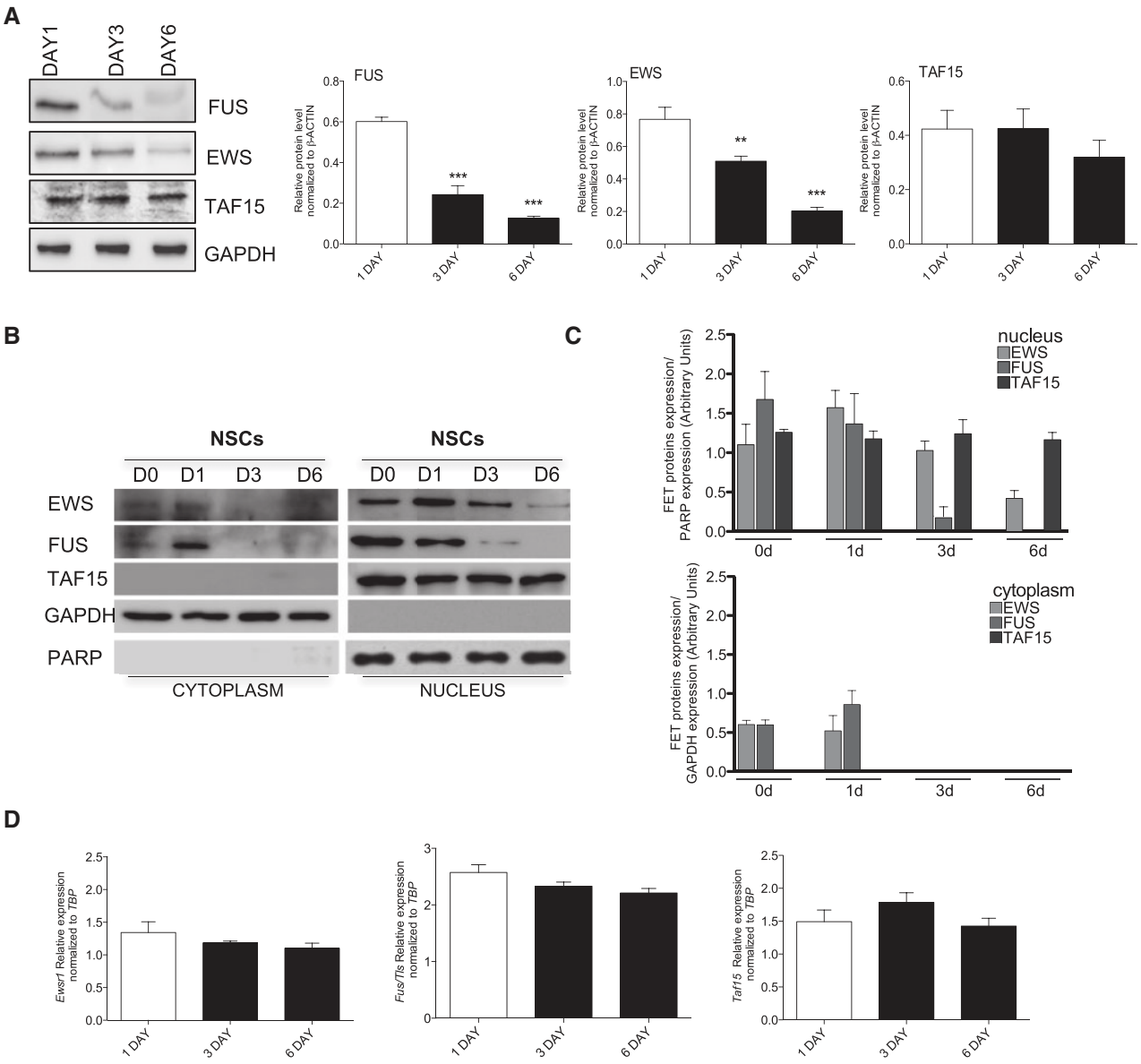

Figure 4. FET expression in differentiating NSCs. (**A**) On the left, western blot analysis of FET proteins during differentiation of NSCs. Total extracts were normalized to GAPDH content. On the right, bar graphs represent densitometric analyses of FET protein expression normalized to GAPDH expression from three independent experiments. Statistical analysis was performed by Student's *t*-test: $^{*}P < 0.05$, $^{**}P < 0.01$, $^{***}P < 0.001$ for each time point vs DAY1. (**B**) Western Blot analysis of FET proteins expression and cellular localization in NSCs cultured under proliferating condition (0d) or after 1-6 days of differentiation (1-6d). GAPDH and PARP expression was used as loading and cytoplasm/nuclear fraction control, respectively. (**C**) Densitometric analysis of FET proteins expression in the nucleus (upper panel) or in the cytoplasm (lower panel) of NSCs cultured in proliferating condition (0d) or during 1-6 days of differentiation (1-6d). (**D**) RT-qPCR analysis to monitor *Fus/Tls*, *Ews* and *Taf15* mRNA expression during differentiation of NSCs mouse brain development. Bar graphs represent densitometric analyses of FET mRNA expression normalized to *Tbp* mRNA levels from three independent experiments. Statistical analysis was performed by Student's *t*-test: $^{*}P < 0.05$, $^{**}P < 0.01$, $^{***}P < 0.001$ for each time point vs DAY1.

currently known. Herein, investigation of the pattern of expression of the three FET proteins during brain development and neuronal differentiation highlighted a distinct temporal and spatial pattern for each protein, with TAF15 being the most constitutively expressed isoform, whereas FUS and EWS expression is regulated at the post-transcriptional level upon differentiation. In particular, we found that miRNAs of the miR-141/200a subfamily repress the expression of both FUS and EWS in differentiating neuronal cells. Thus, our results uncover unique features of expression for each FET protein in the developing mouse brain and identify a miRNA-based post-transcriptional mechanism that controls two of these proteins in neurons.

Expression of FET proteins, and, in particular of FUS and EWS, peaked at stages of intense neurogenesis in the developing cortex and declined after birth, when the differentiation process is almost completed (32). Furthermore, we describe a specific pattern of temporal and spatial expression for each FET protein during brain development, suggesting potential non-overlapping functions for this family of RBPs. In undifferentiated NSCs, FUS and EWS mark both the nucleus and the cytoplasm, whereas TAF15 is exclusively localized in the nucleus, suggesting that they may play a role in

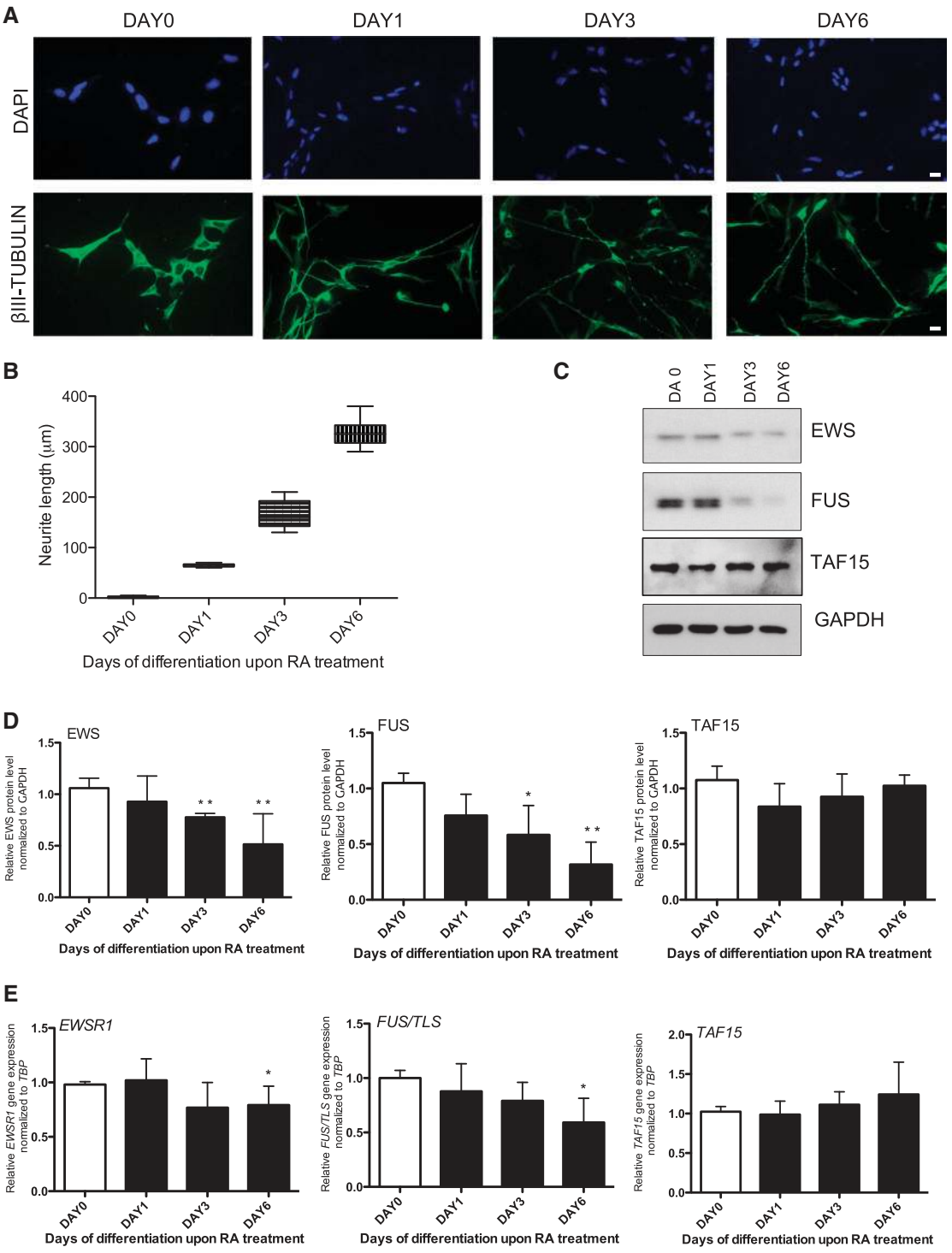

Figure 5. FET expression in retinoic acid induced differentiation of SH-SY5Y cells. (**A**) Cells were seeded on dishes and treated with 10 μM of retinoic acid for the indicated days. Neurite outgrowth was observed beginning at days 0, 1, 3 and 6 of the treatment. Cells were stained with a β-III-Tubulin antibody (green) and DAPI (blue). Scale bar = 25 μm. (**B**) The length of the neurites extending from the SH-SY5Y cells after 0, 1, 3 and 6 days of differentiation were measured by using the ImageJ software and the average length (l) for each day was expressed in a graph ± SD, $n = 3$. Statistical analysis was performed by Student's *t*-test: $^{*}P < 0.05$. The neurite outgrowth upon RA treatment was significantly extensive. D0: $l = 0.459$, $P = 0.765$; D1: $l = 68.82$, $P < 0.01$; D3: $l = 64.33$, $P < 0.01$; D6: $l = 83.32$, $P < 0.01$. (**C**) Western blot analysis of FET protein expression in RA-induced differentiation of SH-SY5Y cells. 10 μg of proteins from SH-SY5Y cell extracts were loaded in each lane of a 10% poly-acrylamide gel. (**D**) Histograms represent the quantification of FET protein normalized to GAPDH from three independent experiments ($n = 3$; mean ± s.d.). In all panels, statistical analysis was performed by Student's *t*-test: $^{*}P < 0.05$, $^{**}P < 0.01$, $^{***}P < 0.001$. (**E**) qPCR analysis showing the levels of *Fus/Tls*, *Ews* and *Taf15* transcripts, normalized for levels of the housekeeping gene *Tbp*. Bars represent mean ± SD from 3 experiments. In all panels, statistical analysis was performed by Student's *t*-test: $^{*}P < 0.05$, $^{**}P < 0.01$, $^{***}P < 0.001$.

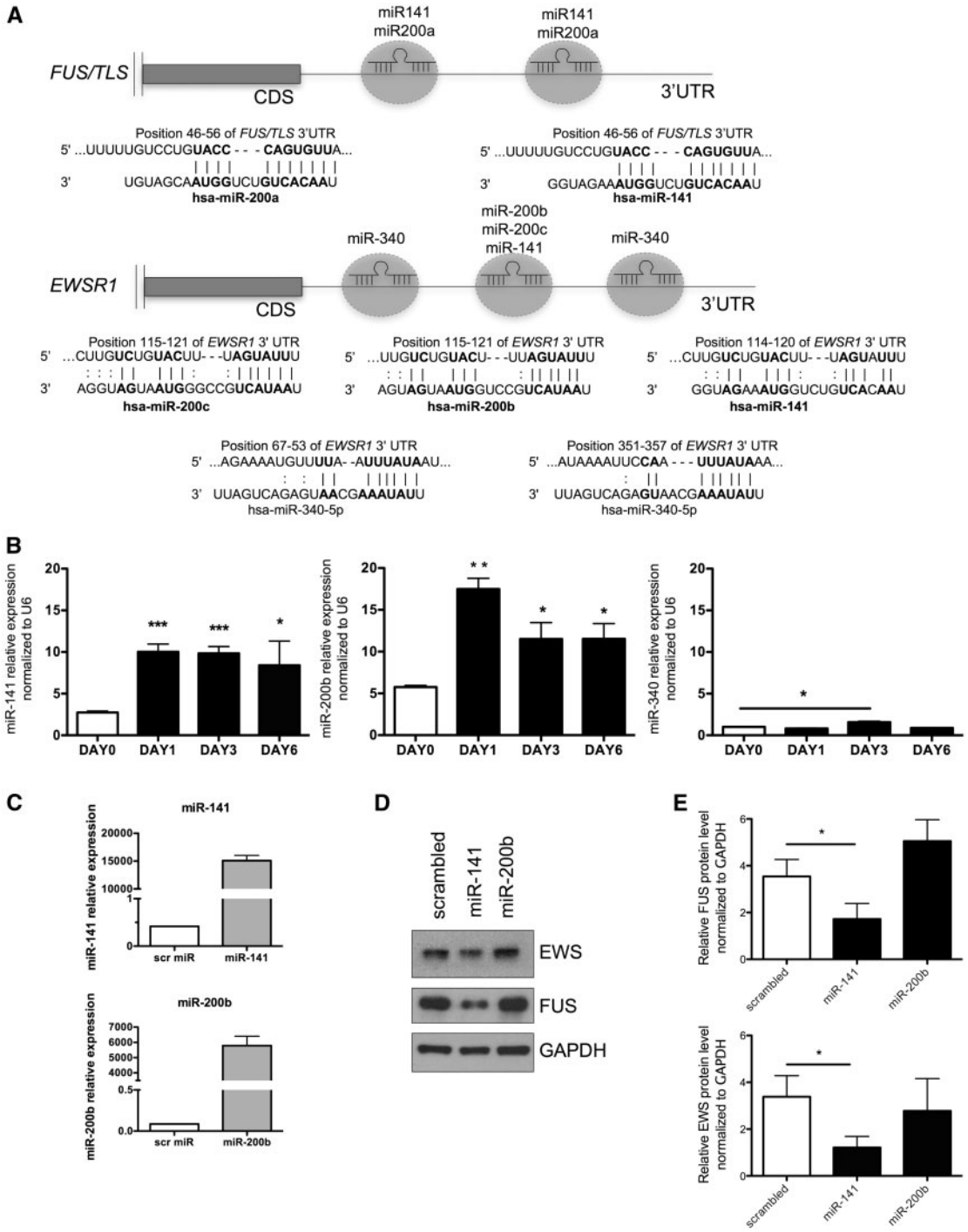

Figure 6. EWS and FUS expression are finely regulated by miR-141 during neural differentiation. (**A**) *In silico* analysis showing the putative miRNA able to bind *FUS* and *EWSR1* 3'UTRs. (**B**) RT-qPCR showing the expression of miR-141, miR-200b and miR340 during SH-SY5Y differentiation. Histograms represent the quantification of the indicated miRNAs normalized to U6 from three independent experiments ($n = 3$; mean ± s.d.). In all panels, statistical analysis was performed by Student's *t*-test: $^{*}P < 0.05$, $^{**}P < 0.01$, $^{***}P < 0.001$. (**C**) RT-qPCR showing the expression levels of miR-141 and miR-200b at 36 h after mimic transfections. Histograms represent the quantification of the indicated miRNAs normalized to U6 from three independent experiments ($n = 3$; mean ± s.d.). (**D**) Representative image of the western blot analysis showing the protein expression of FUS and EWS at 72 h upon miR-141 and miR-200b transfections. Protein expression was calculated by normalizing to GAPDH protein levels. (**E**) Histograms represent the quantification of FUS and EWS protein normalized to GAPDH from three independent experiments ($n = 3$; mean ± s.d.). In all panels, statistical analysis was performed by Student's *t*-test: $^{*}P < 0.05$.

different subcellular compartments. It is unclear what differences in terms of protein architecture could determine such changes in localization, as FET proteins are highly related and share more than 60% of protein similarity (2,3). A putative NLS, consisting in a peptide located in the last 18 amino acid residues of the C-terminal domain (Fig. 2D), is present in all FET proteins and deletion of this region causes their drastic redistribution (41). In addition, FUS contains a predicted nuclear export signal 289–298

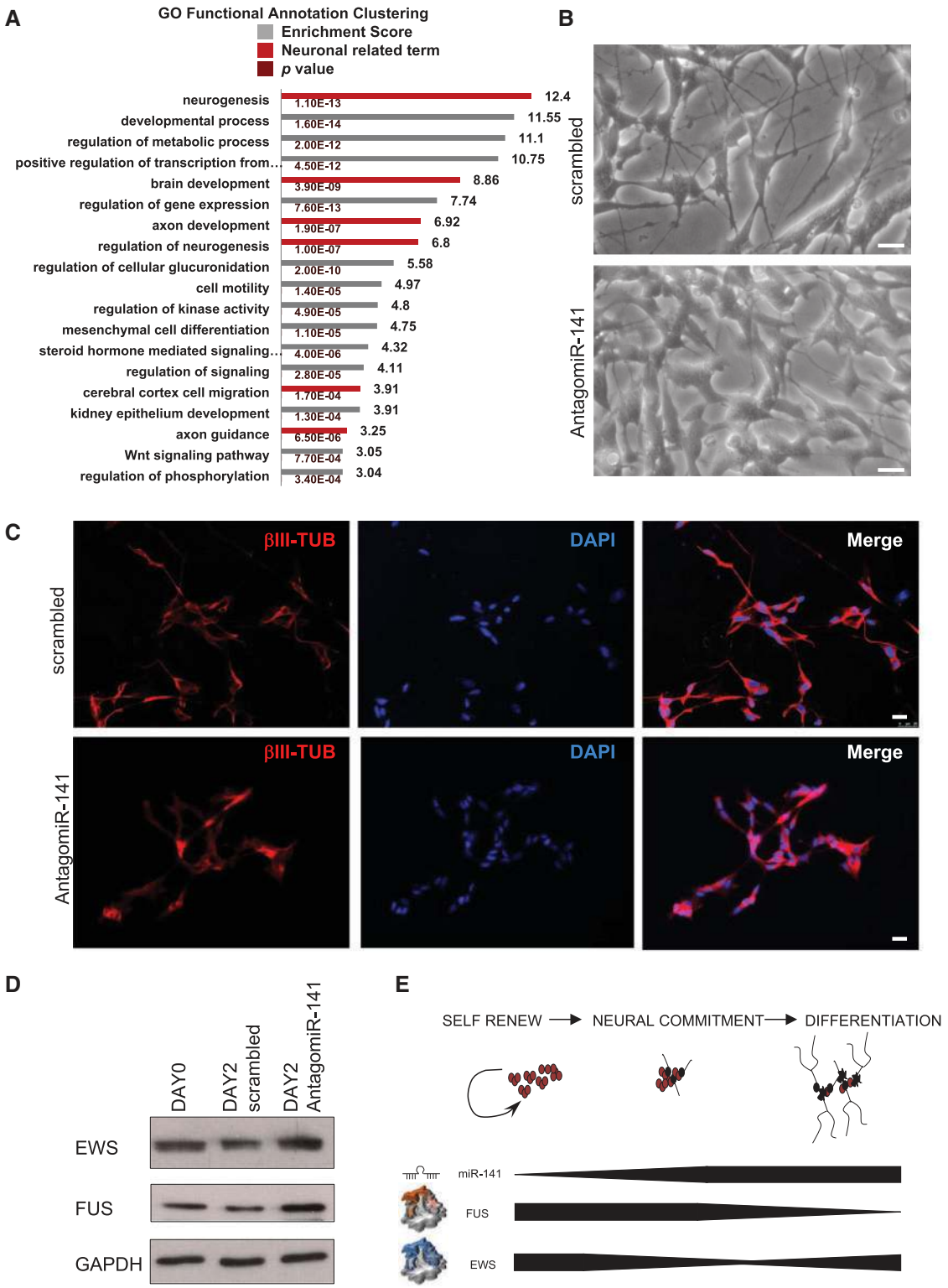

Figure 7. (**A**) Gene ontology functional annotation clustering of miR-141 predicted targets (www.targetscan.org). Histograms represent the overall enrichment score for the group based on the EASE score (a modified Fisher Exact P-Value), set to 0.05 for each term. The higher, the more enriched. The Group Enrichment Score is used to rank the biological significance of each term. Terms are listed for enrichment score ≥ 3. Neuronal related GO terms are filled in red; *p*-values associated with each annotation terms are indicated. (**B**) Representative images in bright field of SH-SY5Y cells transfected with either scrambled or AntagomiR-141 oligonucleotides. 24 h after transfection, cells were treated with 10 μM of Retinoic Acid (RA) to induce differentiation. After 2 days of differentiation cells were harvested. Scale bar = 25 μm. (**C**) Representative images in bright field of SH-SY5Y cells after transfection with either scrambled or AntagomiR-141 oligonucleotides, as in (**B**). After 2 days of differentiation cells were stained with β-III-Tubulin antibody (red) and DAPI (blue). Scale bar = 25 μm. (**D**) Western blot analysis of FET protein expression in SH-SY5Y cells transfected with either scrambled or AntagomiR-141 oligonucleotides. Cells were treated with RA for two days and then harvested. 5 μg of protein extracts were loaded in each lane of a 7% poly-acrylamide gel. Total extracts were normalized to GAPDH. (**E**) Schematic representation of the regulation of FUS and EWS by miR-141 during neural differentiation. Upon neural commitment, miR-141 is upregulated and targets FUS and EWS, thus leading to the down-regulation of FUS and EWS proteins.

(VQGLGENVTI) (42), that is not present in EWS and TAF15 proteins (Fig. 2D) and could contribute, at least in part, to the different behavior of the three FET family members. Importantly, the nucleocytoplasmic shuttling of FUS is crucial to accomplish its role; in fact, interference with this function can contribute to neurodegenerative disease, as demonstrated ALS-linked mutations leading to a predominance of its cytoplasmic localization (21,22,42–46).

During the NSC differentiation process, TAF15 maintains its strong nuclear localization in both astrocytes and neurons with no detectable changes (Fig. 3D), while FUS and EWS expression is almost suppressed in astrocytes (Supplementary Material, Fig. S2). In neurons, FUS and EWS show different patterns of expression. EWS is initially reduced in the early stages of differentiation (day 1 and 3) and partially increases in the more mature, branched neurons at day 6 of differentiation (Fig. 3B, Supplementary Material, Fig. S2). By contrast, FUS expression is still detectable at day 1 of differentiation but it almost disappears in the more differentiated neurons (Fig. 3C; Supplementary Material, Fig. S2). Thus, our results uncover possible non-redundant functions of the FET proteins in different brain compartments as well as within neuronal cells.

The changes in FUS and EWS protein expression were not paralleled by significant differences at the mRNA levels. This observation highlighted the possibility of a post-transcriptional mechanism of regulation of their expression. Post-transcriptional regulation is mediated by both cis-acting sequence elements located on the target RNA and trans-acting regulatory factors, such as RBPs and/or non-coding RNAs, in particular miRNAs (47–49). MiRNAs are small non-coding RNAs that guide the RNA induced silencing complex (RISC) on targets. By regulating the expression of protein-coding genes, miRNAs are involved in almost every biological process in eukaryotes and their dysregulation has been associated with many human diseases (50). MiRNAs also play a pivotal role in neurogenesis (51,52). Dicer depletion in olfactory progenitor cells at embryonic day 9.5 (E9.5), and in particular loss of function of the miR-200 family, reduced the number of neuron-committed progenitor cells and mature neurons (53) and caused disorganization throughout the cortex (54). Moreover, deletion of Dicer in the developing cerebral cortex by E9.5 lead to the reduction of specific miRNAs followed by thinning of the cerebral cortex and increased apoptosis in newborn neurons (55,56). MiRNA depletion can also affect the adult neurogenesis niche. As an example, miR-124 modulates the transitory progression of adult neurogenesis within the subventricular zone (SVZ) by influencing the expression of the transcription factor SOX9 (57). Thus, loss of miRNAs in NSCs profoundly impacts production of neurons. However, whether these defects reflect loss of many miRNAs or a select few is still unclear.

To unravel the mechanism by which FUS and EWS expression is regulated during neuronal differentiation, we used neuroblastoma cells that can be efficiently and homogenously induced to differentiate into a neuronal-like state. Notably, regulation of FET protein expression during differentiation of human neuroblastoma cells recapitulated that observed in primary murine NSCs, including the uncoupling between FET mRNA and protein expression profiles. These findings suggested the existence of evolutionary conserved regulatory signals linked to specific post-transcriptional regulators. Bioinformatics analyses for miRNAs predicted to target their 3'UTRs indicated that miR-141/200a can potentially target FUS, whereas miR-141/200a, miR-200b/200c and miR-340 have the potential to target EWS. We also found that miR-141 and miR-200b are upregulated during RA-induced differentiation of SH-SY5Y cells, whereas miR-340 is not. Interestingly, mimic transfection of miR-141 was sufficient to downregulate both FUS and EWS expression in SH-SY5Y cells, whereas miR-200b did not modulate EWS expression even though it was predicted to bind its 3'UTR. The miR-200 family members are among the most strongly downregulated miRNAs in *Dicer1* conditional KO mice and were previously shown to play a crucial role in the generation and survival of ventral neuronal populations in the murine midbrain/hindbrain by directly targeting the pluripotency factor SOX2 and the cell-cycle regulator E2F3 in neural stem/progenitor cells (58). Thus, posttranscriptional regulation of FUS and EWS by miR-141 might contribute, together with the regulation of SOX2 and E2F3 by the other members of the miR-200 family, to control the transition from a pluripotent progenitor cell to a post-mitotic and more differentiated cell (58,59).

FET proteins can enhance miRNA expression by direct binding to nascent pri-miRNAs on chromatin and facilitating co-transcriptional processing (60–62). In particular, FUS was shown to control miR-141 biogenesis through a regulatory loop in which FUS increases the expression levels of these miRNAs that in turn limit FUS accumulation (63,64). Our results confirm at the protein level the regulation of FUS by miR-141. Although we could not recapitulate directly the regulation by the sole 3'UTR, our data support the hypothesis that EWS expression is also under control of miR-141 in neuronal cells. Furthermore, we show that the FET proteins/miR-141 regulatory loop is set in motion at the onset of neuronal differentiation of precursor cells (Fig. 7E). This fine-tuned control of FUS and EWS concentration in neurons during brain development might have strong physiological relevance, as it has been demonstrated that up-regulation of wild type FUS is sufficient to cause death in motor neuronal NSC34 cells and primary cortical neurons (65), and mutations in the 3'UTR of FUS found in ALS patients resulted into translation de-regulation, overexpression and ALS-related mislocalization of FUS in neuronal cells (66). Remarkably, gene ontology analysis uncovered the enrichment for functional categories involved in neural differentiation and RNA regulation among the putative targets of miR-141 (Fig. 7A). Accordingly, we found that inhibition of miR-141 blocks morphological differentiation of cells into neurons (Fig. 7B and C). These observations suggest that downregulation of FUS and EWS is part of a broader program of neuronal differentiation orchestrated by miR-141. Another interesting finding of our study is the non-redundant function within the miR-200 family during neuron differentiation. Indeed, while miR-200b is strongly up-regulated upon differentiation, like miR-141, it does not modulate FET protein expression. Thus, the activity of miR-200 members may not be interchangeable during neurogenesis and it is likely that each miRNA controls a subset of targets in a specific fashion.

The recent discovery of the implication of FET proteins in neurodegenerative diseases renewed the interest in elucidating their physiological functions. To date, it is still not clear which, if any, endogenous function of FET proteins is involved in the pathogenesis of these diseases. In *Drosophila* loss of the miR-200 homolog (mir-8) results in both excess proliferation and ectopic neuroblast transition (67). Thus, regulation of FUS and EWS expression by miR-141 could contribute, at least in part, to balance neuro-epithelial proliferation and neuroblast formation. Notably, overexpression of FET proteins leads to ALS-related phenotypes. In this scenario, impairment of the regulation of FUS and EWS expression might contribute, at least in part, to create a positive loop of protein production and aggregation, resulting in sequestration of newly produced FUS, together with its RNA targets, into the cytoplasmic aggregates. Since post-transcriptional regulation and translational inhibition of target genes are associated with both physiological neurogenesis and neurodegenerative disorders, our results suggest that proper regulation of FET protein expression by miR-141 is a novel key player in these processes.

Materials and Methods

Animals and neural stem cells isolation and culture

Neural stem cells (NSCs) were isolated from C57/BL6 (Charles River Laboratories, Sulzfeld, Germany) mouse embryos, following the Institutional guidelines of the University of Rome Tor Vergata and the approval of the local Ethical Committee. The age of the embryos was determined according to the staging criteria of Theiler, in which embryonic day 13.5 (E13.5) corresponds to stage 22 (68). E13.5 cerebral cortices were isolated and treated as previously described (34). Briefly, brain tissues were enzymatically digested with Papain (30 U/ml, Worthington, Lakewood, NJ, USA), L-Cysteine (0.24 mg/ml, Sigma-Aldrich St Louis, MO, USA), DNaseI (40 mg/ml, Sigma-Aldrich, St Louis, MO, USA) dissolved in minimum essential medium (MEM, Sigma-Aldrich, St Louis, MO, USA) for 10 min at 37 °C to obtain cell suspensions. Enzymatic activity was stopped by the addition of 1 ml of ovomucoid, containing 1 mg/ml Trypsin inhibitor (Sigma-Aldrich, St. Louis, MO, USA), 50 mg/ml bovine serum albumin (BSA), 40 mg/ml DNaseI in L-15 medium (all reagents from Sigma-Aldrich, St Louis, MO, USA). Cells were then centrifuged and resuspended in neurosphere medium consisting of DMEM:F12 (1:1) (Sigma-Aldrich, St. Louis, MO, USA) containing 0.2 mg/ml L-glutamine (Sigma-Aldrich St Louis, MO, USA), B27 (1 ml/50 ml, Gibco, Life Technologies Ltd, Paisley, UK), penicillin (100 U/ml), streptomycin (100 mg/ml) (all from Lonza, Basel, CH), and supplemented with epidermal growth factor (EGF) and basic fibroblast growth factor (bFGF) (both from EMD Millipore Corporation, Billerica, MA, USA). For the differentiation studies, four-well dishes (Greiner, Kremsmunster, Austria) were coated with poly-ornithine (Sigma-Aldrich, St Louis, MO, USA) in H_2O, and with laminin-1 (Tebu-bio, Offenbach, Germany) in PBS for 1 h each at 37 °C. After several washes, cells were plated at 20000 cells/well density in neurosphere medium containing 1% v/v fetal bovine serum (FBS) and incubated in a humidified atmosphere with 6% CO_2 at 37 °C for 3 days.

Immunofluorescence analysis

NSCs were fixed for 20 min with 4% paraformaldehyde at room temperature and rinsed thrice with PBT1 (phosphate-buffered saline, 1% BSA and 0,1% TritonX100). The primary antibodies were incubated over night at +4 °C the following concentration: mouse anti-Nestin (1:1000) (Millipore, Darmstadt, Germany), mouse anti-b-III-tubulin (1:300) (Sigma-Aldrich, St Louis, MO, USA), rabbit anti-GFAP (glial fibrillary acidic protein) (1:250) (DAKO, Glostrup, Denmark), rabbit anti-FUS (1:300) (ab23439 Abcam), rabbit anti-EWS (1:500) (30) and rabbit anti-TAF15 (1:500) (ab134916 Abcam). After PBS washes, cells were incubated for 1 h with Cy3- (1:500) and FITC-conjugated (1:250) secondary antibodies (Jackson ImmunoResearch Laboratories, Inc. West Grove, PA, USA). Cell nuclei were stained by 4'-6-Diamidino-2-phenylindole (DAPI). Samples were then viewed and photographed by using an inverted microscope (DMI6000B; Leica Geosystems AG, Heerbrugg, CH) equipped with a Neofluar HCX 40.0x/1.25 oil UV objective and acquired using IAS AF Lite software (Leica Microsystems).

Subcellular fractionation of NSCs

Cytoplasmic protein extracts were prepared using hypotonic lysis buffer (Hepes 10 mM, KCl 10 mM, EDTA 0,1 mM, EGTA 0,1 mM, NP-40 0,05% v/v). The extracts were incubated on ice for 15 min and then centrifuged for 15 min at 3000 rpm at 4 °C. After supernatant removal (representing the cytoplasmic protein fraction), nuclear pellet was lysed using nuclei lysis buffer (Hepes 20 mM, NaCl 420 mM, $MgCl_2$ 1,5 mM, Glycerol 20% v/v, Triton X-100 0,05% v/v). Nuclear extracts were incubated on ice for 30' and then centrifuged for 20' at 13000 rpm at 4 °C. All buffers were supplemented with 1 mM dithiothreitol, 10 mM β-glycerophosphate, 0.5 mM Na3VO4, and protease inhibitor cocktail (Sigma-Aldrich).

Isolation of total RNA and RT-qPCR

Total RNA was extracted by using TriPure Isolation Reagent (Roche) according to the manufacturer's instructions and subjected to DNase digestion (Roche). First-strand cDNA was obtained from 1μg of RNA using random hexamer and M-MLV-Reverse Transcriptase (Promega, Italy). Synthesized cDNA corresponding to 25 ng total RNA was used for either conventional-(GoTaq DNA Polymerase, Promega) or quantitative-PCR (SYBR Green Master Mix for Light-Cycler 480, Roche), according to manufacturer's instructions. Primers used for RT-qPCR analyses are listed in the Supplementary Material, Table S1.

For miRNA expression analysis TaqMan method was employed. Briefly, 10 ng of total RNA was reverse-transcribed using TaqMan miRNA reverse transcription kit (Applied Biosystems, 4366596) following manufacturer's instructions. Then 1.3 μl of each miR-specific cDNA was submitted to PCR amplification by using Taqman universal PCR master mix II (Applied Biosystems, 4440044). The following TaqMan miRNA assays were used as probes: hsa-miR-141 (000463), hsa-miR-200b (002251), hsa-miR-340 (002258) and U6 snRNA (001973).

The comparative cycle threshold (Δ ΔCt) method was used to analyze the relative expression levels using TBP or U6 snRNA as internal controls.

Protein extraction and western blot analyses

Total protein extracts were prepared using RIPA buffer supplemented with 1 mM dithiothreitol, 10 mM β-glycerophosphate, 0.5 mM Na_3VO_4, and protease inhibitor cocktail (Sigma-Aldrich) supplemented. The extracts were incubated on ice for 10 min and then centrifuged for 10 min at 12,000 g at 4 °C. Protein quantification was performed by Quick Start Bradford Protein Assay (Bio-Rad). Cell extracts were diluted in Laemmli buffer and boiled for 5 min. Extracted proteins (10–50 μg) were separated on 6 or 10% SDS-PAGE gels and transferred to Hybond-P membranes (GE Healthcare). Membranes were saturated with 5% non-fat dry milk in phosphate-buffered saline (PBS) containing 0.1% Tween-20 for 1 h at room temperature and incubated with the following antibodies and dilutions overnight at 4 °C: rabbit anti-FUS 1:500 (ab23439 Abcam), rabbit anti-EWS 1:1000, rabbit anti-TAF15 1:500 (ab134916 Abcam), mouse anti-beta ACTIN 1:1000 (04-1116 Merk Millipore), mouse anti-GAPDH 1:1000 (919501 BioLegend) and rabbit anti-PARP (sc-1561, Santa Cruz). Secondary anti-mouse or anti-rabbit IgGs conjugated to horseradish peroxidase (Amersham) were incubated with the membranes for 1 h at room temperature at a 1:10000 dilution in PBS containing 0.1% Tween-20. Immunostained bands were detected by a chemiluminescent method (Santa Cruz Biotechnology). Densitometric analysis was performed by ImageJ software.

Cell cultures, transfections and cell extract preparation

Cell cultures, transfections and sample preparation were carried out by standard methods as previously described (31). Briefly,

SH-SY5Y cells were transfected with various combinations of vectors as indicated using Fugene (Promega). For mimic expression, cells were transfected with 50 nM miRNAs (Life-Technologies) using Lipofectamine RNAi Max (Invitrogen) and Opti-MEM medium (Invitrogen) according to manufacturer's instruction.

Luciferase Assay

SH-SY5Y cells were transfected with 1,5 μg of psicheck-wt 3'UTR_FUS, psicheck-wt 3'UTR EWS or psicheck-mut 3'UTR FUS using Lipofectamine 2000 (Invitrogen) reagent and Opti-MEM medium (Invitrogen), according to manufacturer's instruction. After 24 h cells were detached, replated and transfected with 50 nM miRNAs (Life-Technologies) using Lipofectamine RNAi Max (Invitrogen) and Opti-MEM medium (Invitrogen) according to manufacturer's instruction. Luciferase activity was measured by using Dual-Luciferase Reporter Assay system (Promega), following manufacturer's instruction.

Plasmid Constructs

FUS and EWS 3'UTR were amplified from SH-SY5Y cDNA using the following primers: EWS_UTR FW 5'-cagctcgagtcggccctactagatgcaga -3'; EWS_UTR REV 5'- aatgcggccgcccagcagacacacagtgact -3'; FUS_UTR FW 5'- agctcgagcctggctccccaggttct -3'; FUS_UTR REV 5'- aggcggccgccccccatgacagaaaagtttaat -3'. The amplified product was cloned into the NotI and XhoI sites of psicheck ™-2 vector (Promega).

The mutated versions of psicheck-wt 3'UTR FUS were obtained by Site-directed mutagenesis using the following primers: FUS mut FW 5'- gtcctgtacccacccttaccctcgtta -3'; FUS mut REV 5'-taacgagggtaagggtgggtacaggac -3'. The correct nucleotide sequences of amplified products were verified by sequencing of all the generated constructs (Eurofins).

In silico analyses

Target prediction for miRNA binding sites in the 3'UTR of FUS and EWS mRNAs were performed using the miRanda algorithm (http://www.microrna.org/microrna/home.do) (69) and Target Scan algorithm (www.targetscan.org).

Functional gene annotation clustering for miR-141 predicted targets was performed by using DAVID Bioinformatic Database (https://david.ncifcrf.gov/summary.jsp).

Prediction of leucine-rich nuclear export signals (NES) in FET proteins was performed with NetNES1.1 Server, using a combination of neural networks and hidden Markov models (NetNES 1.1 Server http://www.cbs.dtu.dk/services/NetNES/; 70).

Ethics statement

Animal experiments were performed according to protocol number 809_2015PR, following the Institutional guidelines of the Fondazione Santa Lucia and the approval of the Ethical Committee.

Supplementary Material

Supplementary Material is available at *HMG* online.

Acknowledgements

We thank Drs Silvia Galardi and Silvia Ciafré for the kind gift of miR-141 antagomir. N.M. and P.G.G. were supported by a scholarship from Fondazione Umberto Veronesi.

Conflict of Interest statement. None declared.

Funding

Associazione Italiana Ricerca sul Cancro (AIRC IG17278), Worldwide Cancer Research (AICR-UK 14-0333), University of Rome "Foro Italico" (RIC052016), Telethon (GGP14095), Ministry of Health "Ricerca Corrente" and "5x1000 Anno 2014" to Fondazione Santa Lucia.

References

1. Bertolotti, A., Lutz, Y., Heard, D.J., Chambon, P. and Tora, L. (1996) hTAF(II)68, a novel RNA/ssDNA-binding protein with homology to the pro-oncoproteins TLS/FUS and EWS is associated with both TFIID and RNA polymerase II. *embo J.*, **15**, 5022–5031.
2. Tan, A.Y. and Manley, J.L. (2009) The TET family of proteins: functions and roles in disease. *J. Mol. Cell Biol.*, **1**, 82–92.
3. Paronetto, M.P. (2013) Ewing sarcoma protein: a key player in human cancer. *Int. J. Cell Biol.*, **2013**, 642853.
4. Bertolotti, A., Bell, B. and Tora, L. (1999) The N-terminal domain of human TAFII68 displays transactivation and oncogenic properties. *Oncogene*, **18**, 8000–8010.
5. Andersson, M.K., Ståhlberg, A., Arvidsson, Y., Olofsson, A., Semb, H., Stenman, G., Nilsson, O. and Aman, P. (2008) The multifunctional FUS, EWS and TAF15 proto-oncoproteins show cell type-specific expression patterns and involvement in cell spreading and stress response. *BMC Cell Biol.*, **9**, 37.
6. Zinszner, H., Sok, J., Immanuel, D., Yin, Y. and Ron, D. (1997) TLS (FUS) binds RNA in vivo and engages in nucleocytoplasmic shuttling. *J. Cell Sci.*, **110**, 1741–1750.
7. Delattre, O., Zucman, J., Plougastel, B., Desmaze, C., Melot, T., Peter, M., Kovar, H., Joubert, I., de Jong, P. and Rouleau, G. (1992) Gene fusion with an ETS DNA-binding domain caused by chromosome translocation in human tumours. *Nature*, **359**, 162–165.
8. Crozat, A., Aman, P., Mandahl, N. and Ron, D. (1993) Fusion of CHOP to a novel RNA-binding protein in human myxoid liposarcoma. *Nature*, **363**, 640–644.
9. Sjögren, H., Meis-Kindblom, J., Kindblom, L.G., Aman, P. and Stenman, G. (1999) Fusion of the EWS-related gene TAF2N to TEC in extraskeletal myxoid chondrosarcoma. *Cancer Res.*, **59**, 5064–5067.
10. Kovar, H. (2011) Dr. Jekyll and Mr. Hyde: The Two Faces of the FUS/EWS/TAF15 Protein Family. *Sarcoma*, **2011**, 837474.
11. Azuma, M., Embree, L.J., Sabaawy, H. and Hickstein, D.D. (2007) Ewing sarcoma protein ewsr1 maintains mitotic integrity and proneural cell survival in the zebrafish embryo. *PLoS One*, **2**, e979.
12. Fujii, R., Okabe, S., Urushido, T., Inoue, K., Yoshimura, A., Tachibana, T., Nishikawa, T., Hicks, G.G. and Takumi, T. (2005) The RNA binding protein TLS is translocated to dendritic spines by mGluR5 activation and regulates spine morphology. *Curr. Biol.*, **15**, 587–593.
13. Fujii, R. and Takumi, T. (2005) TLS facilitates transport of mRNA encoding an actin-stabilizing protein to dendritic spines. *J. Cell Sci.*, **118**, 5755–5765.

14. Svetoni, F., Frisone, P. and Paronetto, M.P. (2016) Role of FET proteins in neurodegenerative disorders. *RNA Biol.*, **13**, 1089–1102.
15. Kanai, Y., Dohmae, N. and Hirokawa, N. (2004) Kinesin transports RNA: isolation and characterization of an RNA-transporting granule. *Neuron*, **43**, 513–525.
16. Ibrahim, F., Maragkakis, M., Alexiou, P., Maronski, M.A., Dichter, M.A. and Mourelatos, Z. (2013) Identification of in vivo, conserved, TAF15 RNA binding sites reveals the impact of TAF15 on the neuronal transcriptome. *Cell Rep.*, **3**, 301–308.
17. Riggi, N., Cironi, L., Suvà, M.L. and Stamenkovic, I. (2007) Sarcomas: genetics, signalling, and cellular origins. Part 1: The fellowship of TET. *J. Pathol.*, **213**, 4–20.
18. Mackenzie, I.R., Rademakers, R. and Neumann, M. (2010) TDP-43 and FUS in amyotrophic lateral sclerosis and frontotemporal dementia. *Lancet Neurol.*, **9**, 995–1007.
19. Davidson, Y.S., Robinson, A.C., Hu, Q., Mishra, M., Baborie, A., Jaros, E., Perry, R.H., Cairns, N.J., Richardson, A., Gerhard, A. *et al.* (2012) Nuclear carrier and RNA binding proteins in frontotemporal lobar degeneration associated with fused in sarcoma (FUS) pathological changes. *Neuropathol. Appl. Neurobiol.*, **39**, 157–165.
20. Doi, H., Okamura, K., Bauer, P.O., Furukawa, Y., Shimizu, H., Kurosawa, M., Machida, Y., Miyazaki, H., Mitsui, K., Kuroiwa, Y. *et al.* (2008) RNA-binding protein TLS is a major nuclear aggregate-interacting protein in huntingtin exon 1 with expanded polyglutamine-expressing cells. *J. Biol. Chem.*, **283**, 6489–6500.
21. Kwiatkowski, T.J., Bosco, D.A., Leclerc, A.L., Tamrazian, E., Vanderburg, C.R., Russ, C., Davis, A., Gilchrist, J., Kasarskis, E.J., Munsat, T. *et al.* (2009) Mutations in the FUS/TLS gene on chromosome 16 cause familial amyotrophic lateral sclerosis. *Science*, **323**, 1205–1208.
22. Vance, C., Rogelj, B., Hortobágyi, T., De Vos, K.J., Nishimura, A.L., Sreedharan, J., Hu, X., Smith, B., Ruddy, D., Wright, P. *et al.* (2009) Mutations in FUS, an RNA processing protein, cause familial amyotrophic lateral sclerosis type 6. *Science*, **323**, 1208–1211.
23. Ticozzi, N., Vance, C., Leclerc, A.L., Keagle, P., Glass, J.D., McKenna-Yasek, D., Sapp, P.C., Silani, V., Bosco, D.A., Shaw, C.E. *et al.* (2011) Mutational analysis reveals the FUS homolog TAF15 as a candidate gene for familial amyotrophic lateral sclerosis. *Am. J. Med. Genet. B Neuropsychiatr. Genet.*, **156B**, 285–290.
24. Neumann, M., Rademakers, R., Roeber, S., Baker, M., Kretzschmar, H.A. and Mackenzie, I.R. (2009) A new subtype of frontotemporal lobar degeneration with FUS pathology. *Brain*, **132**, 2922–2931.
25. Belly, A., Bodon, G., Blot, B., Bouron, A., Sadoul, R. and Goldberg, Y. (2010) CHMP2B mutants linked to frontotemporal dementia impair maturation of dendritic spines. *J. Cell Sci.*, **123**, 2943–2954.
26. Neumann, M., Bentmann, E., Dormann, D., Jawaid, A., DeJesus-Hernandez, M., Ansorge, O., Roeber, S., Kretzschmar, H.A., Munoz, D.G., Kusaka, H. *et al.* (2011) FET proteins TAF15 and EWS are selective markers that distinguish FTLD with FUS pathology from amyotrophic lateral sclerosis with FUS mutations. *Brain*, **134**, 2595–2609.
27. Wang, W.Y., Pan, L., Su, S.C., Quinn, E.J., Sasaki, M., Jimenez, J.C., Mackenzie, I.R., Huang, E.J. and Tsai, L.H. (2013) Interaction of FUS and HDAC1 regulates DNA damage response and repair in neurons. *Nat. Neurosci.*, **16**, 1383–1391.
28. Li, H., Watford, W., Li, C., Parmelee, A., Bryant, M.A., Deng, C., O'Shea, J. and Lee, S.B. (2007) Ewing sarcoma gene EWS is essential for meiosis and B lymphocyte development. *J. Clin. Invest.*, **117**, 1314–1323.
29. Dutertre, M., Sanchez, G., De Cian, M.C., Barbier, J., Dardenne, E., Gratadou, L., Dujardin, G., Le Jossic-Corcos, C., Corcos, L. and Auboeuf, D. (2010) Cotranscriptional exon skipping in the genotoxic stress response. *Nat. Struct. Mol. Biol.*, **17**, 1358–1366.
30. Paronetto, M.P., Miñana, B. and Valcárcel, J. (2011) The Ewing sarcoma protein regulates DNA damage-induced alternative splicing. *Mol. Cell*, **43**, 353–368.
31. Paronetto, M.P., Bernardis, I., Volpe, E., Bechara, E., Sebestyén, E., Eyras, E. and Valcárcel, J. (2014) Regulation of FAS exon definition and apoptosis by the Ewing sarcoma protein. *Cell Rep.*, **7**, 1211–1226.
32. Taverna, E., Götz, M. and Huttner, W.B. (2014) The cell biology of neurogenesis: toward an understanding of the development and evolution of the neocortex. *Annu. Rev. Cell Dev. Biol.*, **30**, 465–502.
33. Gonçalves, J.T., Schafer, S.T. and Gage, F.H. (2016) Adult Neurogenesis in the Hippocampus: From Stem Cells to Behavior. *Cell*, **167**, 897–914.
34. Bertram, B., Wiese, S. and von Holst, A. (2012) High-efficiency transfection and survival rates of embryonic and adult mouse neural stem cells achieved by electroporation. *J. Neurosci. Methods*, **209**, 420–427.
35. La Rosa, P., Bielli, P., Compagnucci, C., Cesari, E., Volpe, E., Farioli Vecchioli, S. and Sette, C. (2016) Sam68 promotes self-renewal and glycolytic metabolism in mouse neural progenitor cells by modulating Aldh1a3 pre-mRNA 3'-end processing. *Elife*, **5**, e20750.
36. Compagnucci, C., Di Siena, S., Bustamante, M.B., Di Giacomo, D., Di Tommaso, M., Maccarrone, M., Grimaldi, P. and Sette, C. (2013) Type-1 (CB1) cannabinoid receptor promotes neuronal differentiation and maturation of neural stem cells. *PLoS One*, **8**, e54271.
37. Pahlman, S., Ruusala, A.I., Abrahamsson, L., Mattsson, M.E. and Esscher, T. (1984) Retinoic acid-induced differentiation of cultured human neuroblastoma cells: a comparison with phorbolester-induced differentiation. *Cell Differ.*, **14**, 135–144.
38. Kedde, M. and Agami, R. (2008) Interplay between microRNAs and RNA-binding proteins determines developmental processes. *Cell Cycle*, **7**, 899–903.
39. Mongroo, P.S. and andRustgi, A.K. (2010) The role of the miR-200 family in epithelial-mesenchymal transition. *Cancer Biol. Ther.*, **10**, 219–222.
40. Feng, X., Wang, Z., Fillmore, R. and Xi, Y. (2014) MiR-200, a new star miRNA in human cancer. *Cancer Lett.*, **344**, 166–173.
41. Zakaryan, R.P. and Gehring, H. (2006) Identification and characterization of the nuclear localization/retention signal in the EWS Proto-oncoprotein. *J. Mol. Biol.*, **363**, 27–38.
42. Lanson, N.A., Jr, Maltare, A., King, H., Smith, R., Kim, J.H., Taylor, J.P., Lloyd, T.E. and Pandey, U.B. (2011) A Drosophila model of FUS-related neurodegeneration reveals genetic interaction between FUS and TDP-43. *Hum. Mol. Genet.*, **20**, 2510–2523.
43. Bosco, D.A., Lemay, N., Ko, H.K., Zhou, H., Burke, C., Kwiatkowski, T.J., Jr., Sapp, P., McKenna-Yasek, D., Brown, R.H., Jr. and Hayward, L.J. (2010) Mutant FUS proteins that cause amyotrophic lateral sclerosis incorporate into stress granules. *Hum. Mol. Genet.*, **19**, 4160–4175.
44. Dormann, D., Rodde, R., Edbauer, D., Bentmann, E., Fischer, I., Hruscha, A., Than, M.E., Mackenzie, I.R., Capell, A.,

Schmid, B. et al. (2010) ALS-associated fused in sarcoma (FUS) mutations disrupt Transportin-mediated nuclear import. *embo J.*, **29**, 2841–2857.
45. Kino, Y., Washizu, C., Aquilanti, E., Okuno, M., Kurosawa, M., Yamada, M., Doi, H. and Nukina, N. (2011) Intracellular localization and splicing regulation of FUS/TLS are variably affected by amyotrophic lateral sclerosis-linked mutations. *Nucleic Acids Res.*, **39**, 2781–2798.
46. Ito, D., Seki, M., Tsunoda, Y., Uchiyama, H. and Suzuki, N. (2011) Nuclear transport impairment of amyotrophic lateral sclerosis-linked mutations in FUS/TLS. *Ann. Neurol.*, **69**, 152–162.
47. Glisovic, T., Bachorik, J.L., Yong, J. and Dreyfuss, G. (2008) RNA-binding proteins and post-transcriptional gene regulation. *FEBS Lett.*, **582**, 1977–1986.
48. van Kouwenhove, M., Kedde, M. and Agami, R. (2011) MicroRNA regulation by RNA-binding proteins and its implications for cancer. *Nat. Rev. Cancer*, **11**, 644–656.
49. Filipowicz, W., Bhattacharyya, S.N. and Sonenberg, N. (2008) Mechanisms of post-transcriptional regulation by microRNAs: are the answers in sight?. *Nat. Rev. Genet.*, **9**, 102–114.
50. Taft, R.J., Pang, K.C., Mercer, T.R., Dinger, M. and Mattick, J.S. (2010) Non-coding RNAs: regulators of disease. *J. Pathol.*, **220**, 126–139.
51. Filipowicz, W., Jaskiewicz, L., Kolb, F.A. and Pillai, R.S. (2005) Post-transcriptional gene silencing by siRNAs and miRNAs. *Curr. Opin. Struct. Biol.*, **15**, 331–341.
52. Siegel, G., Saba, R. and Schratt, G. (2011) microRNAs in neurons: manifold regulatory roles at the synapse. *Curr. Opin. Genet. Dev.*, **21**, 491–497.
53. Fineberg, S.K., Kosik, K.S. and Davidson, B.L. (2009) MicroRNAs potentiate neural development. *Neuron*, **64**, 303–309.
54. Choi, P.S., Zakhary, L., Choi, W.Y., Caron, S., Alvarez-Saavedra, E., Miska, E.A., McManus, M., Harfe, B., Giraldez, A.J., Horvitz, H.R. et al. (2008) Members of the miRNA-200 family regulate olfactory neurogenesis. *Neuron*, **57**, 41–55.
55. Makeyev, E.V., Zhang, J., Carrasco, M.A. and Maniatis, T. (2007) The MicroRNA miR-124 promotes neuronal differentiation by triggering brain-specific alternative pre-mRNA splicing. *Mol. Cell*, **27**, 435–448.
56. De Pietri Tonelli, D., Pulvers, J.N., Haffner, C., Murchison, E.P., Hannon, G.J. and andHuttner, W.B. (2008) miRNAs are essential for survival and differentiation of newborn neurons but not for expansion of neural progenitors during early neurogenesis in the mouse embryonic neocortex. *Development*, **135**, 3911–3921.
57. Cheng, L.C., Pastrana, E., Tavazoie, M. and Doetsch, F. (2009) miR-124 regulates adult neurogenesis in the subventricular zone stem cell niche. *Nat. Neurosci.*, **12**, 399–408.
58. Peng, C., Li, N., Ng, Y.K., Zhang, J., Meier, F., Theis, F.J., Merkenschlager, M., Chen, W., Wurst, W. and Prakash, N. (2012) A unilateral negative feedback loop between miR-200 microRNAs and Sox2/E2F3 controls neural progenitor cell-cycle exit and differentiation. *J. Neurosci.*, **32**, 13292–13308.
59. Pandey, A., Singh, P., Jauhari, A., Singh, T., Khan, F., Pant, A.B., Parmar, D. and Yadav, S. (2015) Critical role of the miR-200 family in regulating differentiation and proliferation of neurons. *J. Neurochem.*, **133**, 640–652.
60. Gregory, R.I., Yan, K.P., Amuthan, G., Chendrimada, T., Doratotaj, B., Cooch, N. and Shiekhattar, R. (2004) The Microprocessor complex mediates the genesis of microRNAs. *Nature*, **432**, 235–240.
61. Morlando, M., Dini Modigliani, S., Torrelli, G., Rosa, A., Di Carlo, V., Caffarelli, E. and Bozzoni, I. (2012) FUS stimulates microRNA biogenesis by facilitating co-transcriptional Drosha recruitment. *embo J.*, **31**, 4502–4510.
62. Kim, K.Y., Hwang, Y.J., Jung, M.K., Choe, J., Kim, Y., Kim, S., Lee, C.J., Ahn, H., Lee, J., Kowall, N.W. et al. (2014) A multifunctional protein EWS regulates the expression of Drosha and microRNAs. *Cell Death Differ.*, **21**, 136–145.
63. Dini Modigliani, S., Morlando, M., Errichelli, L., Sabatelli, M. and Bozzoni, I. (2014) An ALS-associated mutation in the FUS 3'-UTR disrupts a microRNA-FUS regulatory circuitry. *Nat. Commun.*, **5**, 4335.
64. Pieraccioli, M., Imbastari, F., Antonov, A., Melino, G. and Raschellà, G. (2013) Activation of miR200 by c-Myb depends on ZEB1 expression and miR200 promoter methylation. *Cell Cycle*, **12**, 2309–2320.
65. Suzuki, H. and Matsuoka, M. (2015) Overexpression of nuclear FUS induces neuronal cell death. *Neuroscience*, **287**, 113–124.
66. Sabatelli, M., Moncada, A., Conte, A., Lattante, S., Marangi, G., Luigetti, M., Lucchini, M., Mirabella, M., Romano, A., Del Grande, A. et al. (2013) Mutations in the 3' untranslated region of FUS causing FUS overexpression are associated with amyotrophic lateral sclerosis. *Hum. Mol. Genet.*, **22**, 4748–4755.
67. Morante, J., Vallejo, D.M., Desplan, C. and Dominguez, M. (2013) Conserved miR-8/miR-200 defines a glial niche that controls neuroepithelial expansion and neuroblast transition. *Dev. Cell*, **27**, 174–187.
68. Bard, J.L., Kaufman, M.H., Dubreuil, C., Brune, R.M., Burger, A., Baldock, R.A. and Davidson, D.R. (1998) An internet-accessible database of mouse developmental anatomy based on a systematic nomenclature. *Mech. Dev.*, **74**, 111–120.
69. Betel, D., Wilson, M., Gabow, A., Marks, D.S. and Sander, C. (2008) The microRNA.org resource: targets and expression. *Nucleic Acids Res.*, **36**, D149–D153.
70. la Cour, T., Kiemer, L., Mølgaard, A., Gupta, R., Skriver, K. and Brunak, S. (2004) Analysis and prediction of leucine-rich nuclear export signals. *Protein Eng. Des. Sel.*, **17**, 527–536.